Modelling Saturated Induction Machines with a View to On-line Dynamic Security Analysis

LUCIAN LUPŞA-TĂTARU
Department of Electrical Engineering
Faculty of Electrical Engineering and Computer Science
Transilvania University
Bd. Eroilor No. 29, Braşov, RO-500036
ROMANIA
lucian.lupsa@unitbv.ro lupsa@programmer.net http://www.unitbv.ro

Abstract: - During the dynamic processes, the induction machine, as component part of interconnected power systems, is now exposed to large variations of magnetic stress. To perform an analysis in on-line mode, when the time required for the computation is a crucial consideration, these variations have to be taken into account by means of a dynamic model that has to combine accuracy with structural simplicity. Various dynamic *d*-*q* axis models of induction machine, derived with the purpose of synthesis of the vector-controlled system or with a view to off-line study, come to be inappropriate for the on-line dynamic security assessment. This is mainly due to models complex structure, which incorporates additional saturation-dependent parameters. The approach in literature, wherein the concept of dynamic (differential) inductance predominates over, will be avoided by reconsidering the winding flux linkage state-space model of induction machine. An auxiliary algebraic equation suitable for a solving in relation to magnetizing inductance will be formulated to complete the original structure of flux linkage state-space model. It will be shown that the employment of the well-established Frölich model to describe the machine magnetizing curve makes feasible the magnetizing inductance expressing in terms of only winding flux linkages. Besides, we will advance the procedure of computing the magnetizing inductance when a magnetizing curve piecewise representation based on Frölich type model is employed. The derivation will be carried out without altering the structural equations of the generalised *d*-*q* axis mathematical model of induction machine.

Key-Words: - Modelling, Dynamic Security Analysis, Induction Machine, Main Flux Saturation, Flux Linkage State-space Model, Frölich Model.

1 Introduction

With the increasing emphasis placed on economy, the induction machine is now operated much closer to the security limits [1]-[4]. On the other hand, more and more induction generators are used in variable-speed drives with fast electromagnetic and mechanical transients [5]-[7]. Bus switching for the emergency generators feeding urgent loads leads to large deviation transients. In this context, to support the operating functions, a large number of scenarios must be anticipated and analysed in on-line mode. Decisions are to be made based on the predicted future states of the system [7]-[10].

To date, a large number of contingency cases are solved in the off-line mode to establish operating guidelines, modified by judgement and experience. Since the number of contingency cases to be solved in energy management systems is usually up to a few thousand cases [7], [10], in order to perform the analysis in on-line mode, the time required for the computation is a crucial consideration. With a view to on-line dynamic security assessment, similar to most of electric power components, the induction machine is usually described by means of a linear, reduced-order dynamic model. This is because the implementation of linear models of power system dynamics on parallel or array processors makes the execution of contingency analysis fast enough [10]. However, in the present context, during the dynamic processes, the main flux path (magnetizing circuit) of the induction machine undergoes large variations of the saturation level. To formulate highly accurate dynamic *d*-*q* axis models, these variations have to be taken into account by means of the anhysteretic magnetizing curve [11]-[19], [21], [22]. Having this in view, the attempts to account for main flux path saturation using flux linkages as state variables are rather rare. One can distinguish the model in [15], where the *d*-*q* axis components of magnetizing flux and rotor current space-phasors [23] are selected as state variables. Contribution [16] advances a class of six different mixed current-flux state-space models;

the "generalised flux space-phasor" is conceptually introduced as a linear combination of selected state-space variables and, later, bound to be aligned with the magnetizing current space-phasor. A number of models in [16] are considerably simpler than the well-established winding current state-space model [12], [14], [17], [18] (derived by selecting all *d*-*q* axis winding currents as state variables) and, thus, more convenient for dynamic security assessment.

Notwithstanding, a survey of more or less recent literature devoted to the formulation of induction machine dynamics reveals that various methods of including the main flux saturation effects give rise to complex structures, which incorporate additional saturation-dependent parameters. Essentially, this is due exactly to the manner of selecting the state variables, which has to be in agreement with the aim of the investigation, represented hitherto mostly by the control system synthesis and off-line dynamic simulation. The approach in literature, wherein the concept of saturation-dependent dynamic inductance predominates over, will be shunned by improving the original structure of the flux linkage state-space model. The approach in [19] and [20], materialised in formulation of algebraic equations, which allow the magnetizing current computation when only the values of the *d*-*q* axis winding flux linkages are available, becomes in this case the most suitable one. The treatment in this paper further develops the idea of main flux saturation modelling given in [19]. Unlike [19], wherein the methodology is aimed at magnetizing current computation, this contribution is redirected at disclosing the induction machine magnetizing inductance as a continuous function of the state variables of flux linkage state-space model.

The main stages within the progression of the derivation procedure will be the following:

→ Adoption of the induction machine (winding) flux linkage state-space model in the original pattern, which includes only state differential equations;
→ Replacement of the *d*-*q* axis currents in the magnetizing current expression (magnetizing current space-phasor modulus) by employing appropriate flux-based expressions;
→ Formulation, in a general form, of an auxiliary algebraic equation that allows the magnetizing inductance computing when only the values of *d*-*q* axis winding flux linkages are available;
→ Employing the well-established Frölich model of the anhysteretic magnetizing characteristics [21], [22] to describe the magnetizing curve of the machine, and carrying out a symbolical (analytical) solving of the auxiliary algebraic equation.

2 Starting Point: The Generalised *d-q* Axis Model of Induction Machine

The generalised *d*-*q* axis mathematical model of the induction machine encompasses two distinctive sets of structural equations:
(i) the differential equations, i.e. voltage and motion equations; (ii) the algebraic correlations between the *d*-*q* axis winding flux linkages and *d*-*q* axis winding currents, namely the so-called flux equations, which allow the selection of the *d*-*q* axis state variables in different variants.

In an arbitrary reference frame, the generalised model of a three-phase induction machine is given by the following structural equations [12]-[16]:
(i) the voltage equations as ordinary differential equations:

$$u_{\mathrm{s}d} = R_{\mathrm{s}} i_{\mathrm{s}d} + \frac{\mathrm{d}\psi_{\mathrm{s}d}}{\mathrm{d}t} - \omega_{\mathrm{ref}} \psi_{\mathrm{s}q} , \qquad (1)$$

$$u_{\mathrm{s}q} = R_{\mathrm{s}} i_{\mathrm{s}q} + \frac{\mathrm{d}\psi_{\mathrm{s}q}}{\mathrm{d}t} + \omega_{\mathrm{ref}} \psi_{\mathrm{s}d} , \qquad (2)$$

$$0 = R_{\mathrm{r}} i_{\mathrm{r}d} + \frac{\mathrm{d}\psi_{\mathrm{r}d}}{\mathrm{d}t} - (\omega_{\mathrm{ref}} - \omega_{\mathrm{r}}) \psi_{\mathrm{r}q} , \qquad (3)$$

$$0 = R_{\mathrm{r}} i_{\mathrm{r}q} + \frac{\mathrm{d}\psi_{\mathrm{r}q}}{\mathrm{d}t} + (\omega_{\mathrm{ref}} - \omega_{\mathrm{r}}) \psi_{\mathrm{r}d} , \qquad (4)$$

wherein u, i, ψ denote voltages, currents, and flux linkages, respectively, while subscripts s and r are associated with stator and rotor, respectively. The reference frame velocity is ω_{ref} with respect to the stator. With respect to the rotor, the reference frame velocity is $\omega_{\mathrm{ref}} - \omega_{\mathrm{r}}$, where ω_{r} represents the rotor angular velocity. Notice that the derivation that is to be performed does not require restrictions regarding the reference frame velocity ω_{ref};
(ii) the flux equations as flux linkages-currents algebraic correlations:

$$\psi_{\mathrm{s}d} = L_{\mathrm{s}} i_{\mathrm{s}d} + L_{\mathrm{m}} i_{\mathrm{r}d} = L_{\mathrm{s}\sigma} i_{\mathrm{s}d} + L_{\mathrm{m}} (i_{\mathrm{s}d} + i_{\mathrm{r}d}) , \qquad (5)$$

$$\psi_{\mathrm{s}q} = L_{\mathrm{s}} i_{\mathrm{s}q} + L_{\mathrm{m}} i_{\mathrm{r}q} = L_{\mathrm{s}\sigma} i_{\mathrm{s}q} + L_{\mathrm{m}} (i_{\mathrm{s}q} + i_{\mathrm{r}q}) , \qquad (6)$$

$$\psi_{\mathrm{r}d} = L_{\mathrm{r}} i_{\mathrm{r}d} + L_{\mathrm{m}} i_{\mathrm{s}d} = L_{\mathrm{r}\sigma} i_{\mathrm{r}d} + L_{\mathrm{m}} (i_{\mathrm{s}d} + i_{\mathrm{r}d}) , \qquad (7)$$

$$\psi_{\mathrm{r}q} = L_{\mathrm{r}} i_{\mathrm{r}q} + L_{\mathrm{m}} i_{\mathrm{s}q} = L_{\mathrm{r}\sigma} i_{\mathrm{r}q} + L_{\mathrm{m}} (i_{\mathrm{s}q} + i_{\mathrm{r}q}) , \qquad (8)$$

wherein L_{m} represents the magnetizing inductance, while index σ denotes the stator and rotor leakage inductances.

Notice that rotor quantities are referred to stator.

The machine electromagnetic torque is given by

$$T_{\mathrm{em}} = \frac{3p}{2} (\psi_{\mathrm{s}d} i_{\mathrm{s}q} - \psi_{\mathrm{s}q} i_{\mathrm{s}d}) \qquad (9)$$

wherein p represents the number of pole pairs. The motion (torque) equation [12]-[16] is irrelevant here and is hence omitted in presentation.

3 Mathematical Modelling

3.1 The Original Structure of Winding Flux Linkage State-space Model

Acknowledged formally as being the oldest one, the winding flux linkage state-space model of induction machine is derived by selecting all *d*-*q* axis winding flux linkages as state variables. The model results considerably simpler than the ones with currents interfering as state variables. This is because of the kindly disposed structure of the generalised voltage equations (1)-(4), which incorporate explicitly the winding flux linkages time-related derivatives. To develop the winding flux linkage state-space model, it is necessary to remove the *d*-*q* axis currents from the voltage equations. By solving the system of Eqs. (5)-(8) in relation to *d*-*q* axis currents, the following currents-flux linkages correlations result:

$$i_{sd} = \frac{L_m(\psi_{sd} - \psi_{rd}) + L_{r\sigma}\psi_{sd}}{(L_{s\sigma} + L_{r\sigma})L_m + L_{s\sigma}L_{r\sigma}}, \quad (10)$$

$$i_{sq} = \frac{L_m(\psi_{sq} - \psi_{rq}) + L_{r\sigma}\psi_{sq}}{(L_{s\sigma} + L_{r\sigma})L_m + L_{s\sigma}L_{r\sigma}}, \quad (11)$$

$$i_{rd} = \frac{L_m(\psi_{rd} - \psi_{sd}) + L_{s\sigma}\psi_{rd}}{(L_{s\sigma} + L_{r\sigma})L_m + L_{s\sigma}L_{r\sigma}}, \quad (12)$$

$$i_{rq} = \frac{L_m(\psi_{rq} - \psi_{sq}) + L_{s\sigma}\psi_{rq}}{(L_{s\sigma} + L_{r\sigma})L_m + L_{s\sigma}L_{r\sigma}}. \quad (13)$$

Thus, the crucial point in the course of derivation of the flux linkage state-space model is typified by the reformulation of the voltage equations. Both *d*-axis currents in Eqs. (1), (3), and both *q*-axis currents in Eqs. (2), (4) can easily be replaced by the flux-based expressions (10), (12) and (11), (13), respectively. If one assumes constant machine parameters then the processed voltage equations will provide the flux linkages time-related derivatives just in terms of state variables, i.e. *d*-*q* axis winding flux linkages and rotor angular velocity:

$$\frac{d\psi_{sd}}{dt} = \omega_1\psi_{sd} + \omega_2\psi_{sq} + \omega_3\psi_{rd} + u_{sd},$$

$$\frac{d\psi_{sq}}{dt} = -\omega_2\psi_{sd} + \omega_1\psi_{sq} + \omega_3\psi_{rq} + u_{sq},$$

$$\frac{d\psi_{rd}}{dt} = \omega_4\psi_{sd} + \omega_5\psi_{rd} + \omega_6\psi_{rq},$$

$$\frac{d\psi_{rq}}{dt} = \omega_4\psi_{sq} - \omega_6\psi_{rd} + \omega_5\psi_{rq} \quad (14)$$

wherein the flux linkages coefficients are:

$$\omega_1 = -R_s\frac{L_m + L_{r\sigma}}{(L_{s\sigma} + L_{r\sigma})L_m + L_{s\sigma}L_{r\sigma}} = \text{const.},$$

$$\omega_2 = \omega_{ref},$$

$$\omega_3 = R_s\frac{L_m}{(L_{s\sigma} + L_{r\sigma})L_m + L_{s\sigma}L_{r\sigma}} = \text{const.},$$

$$\omega_4 = R_r\frac{L_m}{(L_{s\sigma} + L_{r\sigma})L_m + L_{s\sigma}L_{r\sigma}} = \text{const.},$$

$$\omega_5 = -R_r\frac{L_m + L_{s\sigma}}{(L_{s\sigma} + L_{r\sigma})L_m + L_{s\sigma}L_{r\sigma}} = \text{const.},$$

$$\omega_6 = \omega_{ref} - \omega_r. \quad (15)$$

Consequently, with constant parameters, the system analysts deal with a system of (ordinary) differential equations, which is exactly the structure needful for benefiting by a numerical integration routine.

3.2 The Auxiliary Equation

We assume that leakage flux saturation and main flux saturation can be treated independently. Since only saturation of the main flux path is discussed, leakage inductances are constants. In contrast, the main flux saturation is to be taken into account by means of the machine magnetizing curve, described by the following non-linearity [11]-[18]:

$$\psi_m = \psi_m(i_m) = L_m(i_m)\cdot i_m \quad (16)$$

wherein the magnetizing flux linkage as well as the magnetizing inductance change to functions of the magnetizing current variable, that is the magnetizing current space-phasor modulus [23]:

$$i_m = \left|\underline{i}_m\right| = \left|\underline{i}_s + \underline{i}_r\right| = \sqrt{i_{md}^2 + i_{mq}^2} = \sqrt{(i_{sd} + i_{rd})^2 + (i_{sq} + i_{rq})^2}. \quad (17)$$

As already pointed, to develop the flux linkage state-space model, we have to replace the *d*-*q* axis currents in voltage equations (1)-(4) by appropriate expressions in terms of the *d*-*q* axis flux linkages, which, in our case, are state variables. However, having in view that the magnetizing inductance is, for the time being, a dependency upon magnetizing current (17), id est:

$$L_m = L_m(i_m) = \psi_m(i_m)/i_m, \quad (18)$$

the absolute mathematical formulation of the flux linkage state-space model cannot be accomplished. If one attempts to include the main flux saturation effects by the traditional manner, i.e. by introducing the magnetizing inductance as a non-linear function of magnetizing current, then the structure of flux linkage state-space model becomes useless for the analyst-programmers. This is due to the fact that magnetizing current (17), which decides the value of magnetizing inductance in the set of flux-based expressions (10)-(13), is given just in terms of *d*-*q* axis currents, which have to be replaced. With such an attempt of accounting for main flux saturation, the time-related derivatives of winding flux linkages would be expressed not only in terms of winding flux linkages but also in terms of *d-q* axis currents, which are not state variables. Obviously, in this case of hypothetical horizon, any procedure of numerical integration would be of no avail. Thus, in order to have recourse to currents-flux linkages correlations (10)-(13), we have to look for a method that allows the magnetizing inductance computation when only the values of the *d-q* axis winding flux linkages are available. Therefor, we proceed to replace the *d-q* axis currents in the magnetizing current expression (17) by considering just the correlations (10)-(13). The following relationships successively result:

$$i_{\mathrm{m}d} = i_{\mathrm{s}d} + i_{\mathrm{r}d} = \frac{L_{\mathrm{r}\sigma}\psi_{\mathrm{s}d} + L_{\mathrm{s}\sigma}\psi_{\mathrm{r}d}}{(L_{\mathrm{s}\sigma} + L_{\mathrm{r}\sigma})\,L_{\mathrm{m}} + L_{\mathrm{s}\sigma}L_{\mathrm{r}\sigma}}\,,$$

$$i_{\mathrm{m}q} = i_{\mathrm{s}q} + i_{\mathrm{r}q} = \frac{L_{\mathrm{r}\sigma}\psi_{\mathrm{s}q} + L_{\mathrm{s}\sigma}\psi_{\mathrm{r}q}}{(L_{\mathrm{s}\sigma} + L_{\mathrm{r}\sigma})\,L_{\mathrm{m}} + L_{\mathrm{s}\sigma}L_{\mathrm{r}\sigma}}\,,$$

$$i_{\mathrm{m}} = \frac{\lambda_{dq}}{L_{\mathrm{m}} + (L_{\mathrm{s}\sigma} + L_{\mathrm{r}\sigma})^{-1}L_{\mathrm{s}\sigma}L_{\mathrm{r}\sigma}} \tag{19}$$

with λ_{dq} (in Weber) as flux-dependent quantity:

$$\lambda_{dq} = \frac{\sqrt{(L_{\mathrm{r}\sigma}\psi_{\mathrm{s}d} + L_{\mathrm{s}\sigma}\psi_{\mathrm{r}d})^2 + (L_{\mathrm{r}\sigma}\psi_{\mathrm{s}q} + L_{\mathrm{s}\sigma}\psi_{\mathrm{r}q})^2}}{L_{\mathrm{s}\sigma} + L_{\mathrm{r}\sigma}}\,. \tag{20}$$

With regard to main flux saturation modelling, it has to be emphasised the generality of relationship (19), which is of a form independent on the way of representing the magnetizing inductance in relation to magnetizing current variable. On the other hand, for a specific representation (18) of the magnetizing inductance, we take for granted the feasibleness of drawing out the magnetizing current as quantity in connection with and varying with the magnetizing inductance (variable). Thus, we additionally have:

$$i_{\mathrm{m}} = g\,(L_{\mathrm{m}})\,. \tag{21}$$

The generalised relationship (19) coupled with a specific dependency (21) bring forth an auxiliary algebraic equation, its unknown being exactly the magnetizing inductance:

$$\frac{\lambda_{dq}}{L_{\mathrm{m}} + (L_{\mathrm{s}\sigma} + L_{\mathrm{r}\sigma})^{-1}L_{\mathrm{s}\sigma}L_{\mathrm{r}\sigma}} = g\,(L_{\mathrm{m}})\,. \tag{22}$$

Supposing that a function of type (21), varying with magnetizing inductance, makes feasible the symbolical (analytical) solving of auxiliary equation (22), the magnetizing inductance results as function of the flux-dependent quantity (20), i.e. as function of the *d-q* axis flux linkages, which are just state variables. To emphasise this, we simply set down:

$$L_{\mathrm{m}} = f\,(\lambda_{dq})\,. \tag{23}$$

With a dependency of type (23), the inclusion of the effects of the main flux path saturation remains just a straightforward task-work. Indeed, with the main flux saturation effects taken into consideration by means of a dependency of the type (23), the *d-q* axis currents (10)-(13) are preserved as functions of *d-q* axis winding flux linkages:

$$i_{\mathrm{s}d} = f_{11}(\psi_{\mathrm{s}d}, \psi_{\mathrm{s}q}, \psi_{\mathrm{r}d}, \psi_{\mathrm{r}q}) = \frac{f\,(\lambda_{dq})\cdot(\psi_{\mathrm{s}d} - \psi_{\mathrm{r}d}) + L_{\mathrm{r}\sigma}\psi_{\mathrm{s}d}}{(L_{\mathrm{s}\sigma} + L_{\mathrm{r}\sigma})\cdot f\,(\lambda_{dq}) + L_{\mathrm{s}\sigma}L_{\mathrm{r}\sigma}}\,, \tag{24}$$

$$i_{\mathrm{s}q} = f_{12}(\psi_{\mathrm{s}d}, \psi_{\mathrm{s}q}, \psi_{\mathrm{r}d}, \psi_{\mathrm{r}q}) = \frac{f\,(\lambda_{dq})\cdot(\psi_{\mathrm{s}q} - \psi_{\mathrm{r}q}) + L_{\mathrm{r}\sigma}\psi_{\mathrm{s}q}}{(L_{\mathrm{s}\sigma} + L_{\mathrm{r}\sigma})\cdot f\,(\lambda_{dq}) + L_{\mathrm{s}\sigma}L_{\mathrm{r}\sigma}}\,, \tag{25}$$

$$i_{\mathrm{r}d} = f_{21}(\psi_{\mathrm{s}d}, \psi_{\mathrm{s}q}, \psi_{\mathrm{r}d}, \psi_{\mathrm{r}q}) = \frac{f\,(\lambda_{dq})\cdot(\psi_{\mathrm{r}d} - \psi_{\mathrm{s}d}) + L_{\mathrm{s}\sigma}\psi_{\mathrm{r}d}}{(L_{\mathrm{s}\sigma} + L_{\mathrm{r}\sigma})\cdot f\,(\lambda_{dq}) + L_{\mathrm{s}\sigma}L_{\mathrm{r}\sigma}}\,, \tag{26}$$

$$i_{\mathrm{r}q} = f_{22}(\psi_{\mathrm{s}d}, \psi_{\mathrm{s}q}, \psi_{\mathrm{r}d}, \psi_{\mathrm{r}q}) = \frac{f\,(\lambda_{dq})\cdot(\psi_{\mathrm{r}q} - \psi_{\mathrm{s}q}) + L_{\mathrm{s}\sigma}\psi_{\mathrm{r}q}}{(L_{\mathrm{s}\sigma} + L_{\mathrm{r}\sigma})\cdot f\,(\lambda_{dq}) + L_{\mathrm{s}\sigma}L_{\mathrm{r}\sigma}}\,. \tag{27}$$

As a consequence, the replacement of the *d-q* axis currents in the generalised voltage equations (1)-(4) by employing the evolved correlations (24)-(27) will preserve the flux linkages derivatives as expressions in terms of state variables of the original winding flux linkage state-space model:

$$\frac{\mathrm{d}\psi_{\mathrm{s}d}}{\mathrm{d}t} = -R_{\mathrm{s}}\cdot f_{11}(\psi_{\mathrm{s}d}, \psi_{\mathrm{s}q}, \psi_{\mathrm{r}d}, \psi_{\mathrm{r}q}) + \omega_{\mathrm{ref}}\psi_{\mathrm{s}q} + u_{\mathrm{s}d}\,, \tag{28}$$

$$\frac{\mathrm{d}\psi_{\mathrm{s}q}}{\mathrm{d}t} = -R_{\mathrm{s}}\cdot f_{12}(\psi_{\mathrm{s}d}, \psi_{\mathrm{s}q}, \psi_{\mathrm{r}d}, \psi_{\mathrm{r}q}) - \omega_{\mathrm{ref}}\psi_{\mathrm{s}d} + u_{\mathrm{s}q}\,, \tag{29}$$

$$\frac{\mathrm{d}\psi_{\mathrm{r}d}}{\mathrm{d}t} = -R_{\mathrm{r}}\cdot f_{21}(\psi_{\mathrm{s}d}, \psi_{\mathrm{s}q}, \psi_{\mathrm{r}d}, \psi_{\mathrm{r}q}) + (\omega_{\mathrm{ref}} - \omega_{\mathrm{r}})\psi_{\mathrm{r}q}\,, \tag{30}$$

$$\frac{\mathrm{d}\psi_{\mathrm{r}q}}{\mathrm{d}t} = -R_{\mathrm{r}}\cdot f_{22}(\psi_{\mathrm{s}d}, \psi_{\mathrm{s}q}, \psi_{\mathrm{r}d}, \psi_{\mathrm{r}q}) - (\omega_{\mathrm{ref}} - \omega_{\mathrm{r}})\psi_{\mathrm{r}d}\,. \tag{31}$$

Thus, with the effects of the main flux saturation incorporated by means of a non-linearity of the type (23), any derived structure that obeys the evolved form (28)-(31) can lightly be exploited by benefiting by a numerical integration routine [24]-[26].

3.3 Frölich Model of Magnetizing Curve

With a view to off-line analysis, to approximate the magnetizing curve of induction machine, it is in use to call a dedicated curve fitting routine, which is geared toward returning an elaborate differentiable function. However, the evaluation of the returned expression could become very time consuming if the analysis has to be carried out in on-line mode. Although the computer hardware and programming languages are momentous for maximizing execution speed, they do not represent industrial arts we can change on a day-to-day basis. In comparison, what we do implement can be changed at any time, and can drastically affect how long the software blocks will require to execute. In this context, with a view to the on-line assessment, the power system analysts should avoid the using of transcendental functions (e.g. logarithm, trigonometric, hyperbolic functions) for controlling the magnetizing curve fitting. Since the transcendental functions are implemented as a series of additions, subtractions and multiplications, their expressions require at the least ten times longer to evaluate than a single multiplication. Besides, most programming languages only provide a few built-in transcendental functions and expect the analyst-programmers to implement the others by means of several extra calculations.

With the purpose of describing the anhysteretic magnetizing characteristics, it is generally accepted that a good mutual concession between accuracy and the simplicity of the expressing is attained by employing the Frölich model [21], [22] that is given by means of the following rational function:

$$\psi_{\mathrm{m}}(i_{\mathrm{m}}) = i_{\mathrm{m}} / (\alpha + \beta i_{\mathrm{m}}) \;; \quad \alpha > 0\,,\; \beta > 0\,. \tag{32}$$

One perceives that for low values of magnetizing current variable, the magnetizing inductance:

$$L_{\mathrm{m}}(i_{\mathrm{m}}) = (\alpha + \beta i_{\mathrm{m}})^{-1} \tag{33}$$

approaches to the unsaturated value that is inversely proportional to parameter α of the Frölich model, while at high values of magnetizing current variable, the magnetizing flux approaches to saturation:

$$\begin{cases} \lim\limits_{i_{\mathrm{m}} \to 0} L_{\mathrm{m}}(i_{\mathrm{m}}) = \alpha^{-1} \\ \lim\limits_{i_{\mathrm{m}} \to \infty} \psi_{\mathrm{m}}(i_{\mathrm{m}}) = \beta^{-1} \end{cases}$$

From the specific representation (33) of magnetizing inductance, we straightforwardly draw out:

$$i_{\mathrm{m}} = g(L_{\mathrm{m}}) = (1 - \alpha L_{\mathrm{m}}) / (\beta L_{\mathrm{m}})\,. \tag{34}$$

3.4 Magnetizing Inductance Expressing in Terms of State Variables

With magnetizing current (34), connected with and varying with magnetizing inductance, the auxiliary equation (22) becomes:

$$\frac{\lambda_{dq}}{L_{\mathrm{m}} + (L_{\mathrm{s\sigma}} + L_{\mathrm{r\sigma}})^{-1} L_{\mathrm{s\sigma}} L_{\mathrm{r\sigma}}} = \frac{1 - \alpha L_{\mathrm{m}}}{\beta L_{\mathrm{m}}}\,.$$

Thus, in this case, the auxiliary equation comes into sight as a second order algebraic one:

$$(L_{\mathrm{s\sigma}} + L_{\mathrm{r\sigma}})^{-1} L_{\mathrm{s\sigma}} L_{\mathrm{r\sigma}} = \text{const.} = b(\lambda_{dq}) \cdot L_{\mathrm{m}} + \alpha L_{\mathrm{m}}^2 \tag{35}$$

with b as the flux-dependent coefficient:

$$b(\lambda_{dq}) \equiv \alpha (L_{\mathrm{s\sigma}} + L_{\mathrm{r\sigma}})^{-1} L_{\mathrm{s\sigma}} L_{\mathrm{r\sigma}} - 1 + \beta \lambda_{dq}\,.$$

The positive defined solution of Eq. (35) can be brought before in the following algebraic form:

$$L_{\mathrm{m}} = f(\lambda_{dq}) = \sqrt{c_0 + (c_1 + c_2 \lambda_{dq})^2} - c_1 - c_2 \lambda_{dq} \tag{36}$$

wherein quantities:

$$c_0 = \alpha^{-1} (L_{\mathrm{s\sigma}} + L_{\mathrm{r\sigma}})^{-1} L_{\mathrm{s\sigma}} L_{\mathrm{r\sigma}}\,, \tag{37}$$

$$c_1 = 0.5 (L_{\mathrm{s\sigma}} + L_{\mathrm{r\sigma}})^{-1} L_{\mathrm{s\sigma}} L_{\mathrm{r\sigma}} - 0.5/\alpha\,, \tag{38}$$

$$c_2 = 0.5 \beta / \alpha \tag{39}$$

depend solely on leakage inductances and Frölich model parameters and, consequently, designate a set of constants. Relation (36) yields the magnetizing inductance as function of flux-dependent quantity (20), i.e. in terms of winding flux linkages, which are just state variables. Eqs. (36) and (20) disclose:

$$L_{\mathrm{m}} = \sqrt{c_0 + (c_1 + c_2' \lambda_{dq}')^2} - c_1 - c_2' \lambda_{dq}'\,;$$

$$\lambda_{dq}' = \sqrt{\left(\begin{bmatrix} L_{\mathrm{r\sigma}} \\ L_{\mathrm{s\sigma}} \end{bmatrix}^{\mathrm{T}} \begin{bmatrix} \psi_{\mathrm{s}d} \\ \psi_{\mathrm{r}d} \end{bmatrix} \right)^2 + \left(\begin{bmatrix} L_{\mathrm{r\sigma}} \\ L_{\mathrm{s\sigma}} \end{bmatrix}^{\mathrm{T}} \begin{bmatrix} \psi_{\mathrm{s}q} \\ \psi_{\mathrm{r}q} \end{bmatrix} \right)^2}\,,$$

$$c_2' = (L_{\mathrm{s\sigma}} + L_{\mathrm{r\sigma}})^{-1} c_2 = \text{const.}$$

In this context, non-linearity (36) is to be used as a replacement for non-linearity (33) that traditionally yields the magnetizing inductance as function of magnetizing current (17), i.e. in terms of *d*-*q* axis currents. Thus, with magnetizing inductance (36), the *d*-*q* axis currents and the time-related derivatives of *d*-*q* axis winding flux linkages get their evolved expressions in terms of only state variables, i.e. the expressions (24)-(27) and (28)-(31), respectively.

Besides the fact that the dynamic (differential) inductance does not interfere, the encompassing of two parameters within the Frölich model (32) makes allowable a convenient method for the anhysteretic magnetizing curve fitting. More precisely, one can simply employ the Frölich type model to construct a continuous piecewise representation made up of n constitutive segments:

$$\psi_{\mathrm{m}}(i_{\mathrm{m}}) = \begin{cases} i_{\mathrm{m}} / (\alpha_0 + \beta_0 i_{\mathrm{m}})\,; & 0 \le i_{\mathrm{m}} < i_{\mathrm{m},1} \\ i_{\mathrm{m}} / (\alpha_1 + \beta_1 i_{\mathrm{m}})\,; & i_{\mathrm{m},1} \le i_{\mathrm{m}} < i_{\mathrm{m},2} \\ \vdots & \vdots \\ i_{\mathrm{m}} / (\alpha_k + \beta_k i_{\mathrm{m}})\,; & i_{\mathrm{m},k} \le i_{\mathrm{m}} < i_{\mathrm{m},k+1} \\ \vdots & \vdots \\ i_{\mathrm{m}} / (\alpha_{n-1} + \beta_{n-1} i_{\mathrm{m}})\,; & i_{\mathrm{m},n-1} \le i_{\mathrm{m}} \le i_{\mathrm{m},n} \end{cases} \tag{40}$$

where each pair of parameters α_k and β_k relies on the sampled points $(i_{\mathrm{m},k}, \psi_{\mathrm{m},k})$ and $(i_{\mathrm{m},k+1}, \psi_{\mathrm{m},k+1})$ as follows:

$\alpha_0 = i_{\mathrm{m},1} / \psi_{\mathrm{m},1}$, $\beta_0 = 0$,

simply agreed to a linear interpolation, and further:

$$\alpha_k = \frac{\psi_{\mathrm{m},k+1} - \psi_{\mathrm{m},k}}{\psi_{\mathrm{m},k}\,\psi_{\mathrm{m},k+1}} \frac{i_{\mathrm{m},k}\, i_{\mathrm{m},k+1}}{i_{\mathrm{m},k+1} - i_{\mathrm{m},k}} > 0\,;\ k \neq 0\,,$$

$$\beta_k = \frac{1}{\psi_{\mathrm{m},k}\,\psi_{\mathrm{m},k+1}} \frac{\psi_{\mathrm{m},k}\, i_{\mathrm{m},k+1} - \psi_{\mathrm{m},k+1}\, i_{\mathrm{m},k}}{i_{\mathrm{m},k+1} - i_{\mathrm{m},k}}\,;\ k \neq 0\,.$$

It is quite obvious that if one employs a piecewise approximation of type (40) instead of the Frölich model (32), the accuracy of the magnetizing curve representation can lightly be controlled whatever the specified limit. If (40) is being considered then the magnetizing inductance will result also as piecewise approximation but in relation to the flux-dependent quantity (20), with the mention that each piecewise segment will be accordingly described by means of a non-linearity of the type (36). Thus:

$$L_{\mathrm{m}} = f(\lambda_{dq}) = \begin{cases} f_0(\lambda_{dq})\,; & \lambda_{dq,0} \le \lambda_{dq} < \lambda_{dq,1} \\ f_1(\lambda_{dq})\,; & \lambda_{dq,1} \le \lambda_{dq} < \lambda_{dq,2} \\ \vdots & \vdots \\ f_k(\lambda_{dq})\,; & \lambda_{dq,k} \le \lambda_{dq} < \lambda_{dq,k+1} \\ \vdots & \vdots \\ f_{n-1}(\lambda_{dq})\,; & \lambda_{dq,n-1} \le \lambda_{dq} \le \lambda_{dq,n} \end{cases} \tag{41}$$

wherein, for $k \in [0,\, n-1]$:

$$f_k(\lambda_{dq}) = \sqrt{c_{0,k} + (c_{1,k} + c_{2,k}\,\lambda_{dq})^2} - c_{1,k} - c_{2,k}\,\lambda_{dq}\,;$$

$$\begin{cases} c_{0,k} = \alpha_k^{-1} (L_{\mathrm{s\sigma}} + L_{\mathrm{r\sigma}})^{-1} L_{\mathrm{s\sigma}} L_{\mathrm{r\sigma}}\,, \\ c_{1,k} = 0.5 (L_{\mathrm{s\sigma}} + L_{\mathrm{r\sigma}})^{-1} L_{\mathrm{s\sigma}} L_{\mathrm{r\sigma}} - 0.5/\alpha_k\,, \\ c_{2,k} = 0.5 \beta_k / \alpha_k \end{cases}$$

and, in accordance to Eq. (19), for $k \in [0,\, n]$:

$$\lambda_{dq,k} = \psi_{\mathrm{m},k} + (L_{\mathrm{s\sigma}} + L_{\mathrm{r\sigma}})^{-1} L_{\mathrm{s\sigma}} L_{\mathrm{r\sigma}} \cdot i_{\mathrm{m},k}\,.$$

The results in this subsection suggest that structure (28)-(31) can be applied in conjunction with Frölich model, as well as in conjunction with a piecewise construct based on the Frölich type model (32).

3.5 The Improved Structure of Winding Flux Linkage State-space Model

The derivation in subsection 3.2 shows the course to receiving a winding flux linkage state-space model with the main flux saturation effects incorporated by means of a dependency of the type (23). The state equations (28)-(31) are advanced in the most general form, remaining valid for any dependency described by Eq. (23). In the previous subsection, dependency (23) is made available by employing Frölich model of magnetizing curve as well as by employment of a magnetizing curve piecewise representation based on the Frölich type model. This section deals with the improved structure of the winding flux linkage state-space model in the developed form. This is to be obtained by gathering the results in subsections 3.2 and 3.4. The electromagnetic torque (9) can be expressed in terms of winding flux linkages using correlations (24), (25) to replace the stator *d-q* axis currents (**Appendix A**). Hence, the motion (toque) equation will be omitted in presentation.

Eqs. (28)-(31) can be expanded by employing the correlations (24)-(27) in which dependency (23) can now be given by Eq. (36) or Eq. (41). One obtains:

$$\begin{aligned}
\frac{\mathrm{d}\psi_{\mathrm{s}d}}{\mathrm{d}t} &= -R_{\mathrm{s}} \frac{f(\lambda_{dq}) \cdot (\psi_{\mathrm{s}d} - \psi_{\mathrm{r}d}) + L_{\mathrm{r\sigma}} \psi_{\mathrm{s}d}}{(L_{\mathrm{s\sigma}} + L_{\mathrm{r\sigma}}) \cdot f(\lambda_{dq}) + L_{\mathrm{s\sigma}} L_{\mathrm{r\sigma}}} + \omega_{\mathrm{ref}} \psi_{\mathrm{s}q} + u_{\mathrm{s}d}\,, \\
\frac{\mathrm{d}\psi_{\mathrm{s}q}}{\mathrm{d}t} &= -R_{\mathrm{s}} \frac{f(\lambda_{dq}) \cdot (\psi_{\mathrm{s}q} - \psi_{\mathrm{r}q}) + L_{\mathrm{r\sigma}} \psi_{\mathrm{s}q}}{(L_{\mathrm{s\sigma}} + L_{\mathrm{r\sigma}}) \cdot f(\lambda_{dq}) + L_{\mathrm{s\sigma}} L_{\mathrm{r\sigma}}} - \omega_{\mathrm{ref}} \psi_{\mathrm{s}d} + u_{\mathrm{s}q}\,, \\
\frac{\mathrm{d}\psi_{\mathrm{r}d}}{\mathrm{d}t} &= -R_{\mathrm{r}} \frac{f(\lambda_{dq}) \cdot (\psi_{\mathrm{r}d} - \psi_{\mathrm{s}d}) + L_{\mathrm{s\sigma}} \psi_{\mathrm{r}d}}{(L_{\mathrm{s\sigma}} + L_{\mathrm{r\sigma}}) \cdot f(\lambda_{dq}) + L_{\mathrm{s\sigma}} L_{\mathrm{r\sigma}}} + (\omega_{\mathrm{ref}} - \omega_{\mathrm{r}}) \psi_{\mathrm{r}q}\,, \\
\frac{\mathrm{d}\psi_{\mathrm{r}q}}{\mathrm{d}t} &= -R_{\mathrm{r}} \frac{f(\lambda_{dq}) \cdot (\psi_{\mathrm{r}q} - \psi_{\mathrm{s}q}) + L_{\mathrm{s\sigma}} \psi_{\mathrm{r}q}}{(L_{\mathrm{s\sigma}} + L_{\mathrm{r\sigma}}) \cdot f(\lambda_{dq}) + L_{\mathrm{s\sigma}} L_{\mathrm{r\sigma}}} - (\omega_{\mathrm{ref}} - \omega_{\mathrm{r}}) \psi_{\mathrm{r}d}\,,
\end{aligned} \tag{42}$$

wherein it is possible to have:

$$f(\lambda_{dq}) = \sqrt{c_0 + (c_1 + c_2\,\lambda_{dq})^2} - c_1 - c_2\,\lambda_{dq}$$

if the dependency given by (36) is implemented, or

$$f(\lambda_{dq}) = \sqrt{c_{0,k} + (c_{1,k} + c_{2,k}\,\lambda_{dq})^2} - c_{1,k} - c_{2,k}\,\lambda_{dq}$$

if one implements a piecewise construct of type (41) and the present value of the flux-dependent quantity (20) is detected within the subinterval of extremities $\lambda_{dq,k}$ and $\lambda_{dq,k+1}$. In comparison with the situation of implementing dependency (36), implementation of a piecewise representation given by (41) expects the analyst-programmer to provide a way to change the program flow in order to select the appropriate piecewise segment. This plainly requires a loop that always executes once, e.g. a "repeat…until" looping construct [27], [28] to detect the subinterval wherein the present value of quantity (20) is contained.

Closer inspection of derived structure (42) shows that the flux linkages coefficients, which in original structure (14) have constant values, come now to be saturation-dependent but by means of quantity (20) only, in accordance with Eq. (36) or Eq. (41):

$$\omega_1 \leftarrow -R_\mathrm{s}\,\frac{f(\lambda_{dq}) + L_{\mathrm{r}\sigma}}{(L_{\mathrm{s}\sigma}+L_{\mathrm{r}\sigma})\cdot f(\lambda_{dq}) + L_{\mathrm{s}\sigma}L_{\mathrm{r}\sigma}}\,,$$

$$\omega_3 \leftarrow R_\mathrm{s}\,\frac{f(\lambda_{dq})}{(L_{\mathrm{s}\sigma}+L_{\mathrm{r}\sigma})\cdot f(\lambda_{dq}) + L_{\mathrm{s}\sigma}L_{\mathrm{r}\sigma}}\,,$$

$$\omega_4 \leftarrow R_\mathrm{r}\,\frac{f(\lambda_{dq})}{(L_{\mathrm{s}\sigma}+L_{\mathrm{r}\sigma})\cdot f(\lambda_{dq}) + L_{\mathrm{s}\sigma}L_{\mathrm{r}\sigma}}\,,$$

$$\omega_5 \leftarrow -R_\mathrm{r}\,\frac{f(\lambda_{dq}) + L_{\mathrm{s}\sigma}}{(L_{\mathrm{s}\sigma}+L_{\mathrm{r}\sigma})\cdot f(\lambda_{dq}) + L_{\mathrm{s}\sigma}L_{\mathrm{r}\sigma}}\,. \qquad (43)$$

Having in view that (41) is composed only of pieces of the type (36), we may expand:

$$\omega_1 \leftarrow \omega_1(\lambda_{dq}) = -R_\mathrm{s}\Big(\sqrt{c_0 + (c_1 + c_2\lambda_{dq})^2} - c_1 - c_2\lambda_{dq} + L_{\mathrm{r}\sigma}\Big)\Big/\Big[(L_{\mathrm{s}\sigma}+L_{\mathrm{r}\sigma})\cdot\Big(\sqrt{c_0+(c_1+c_2\lambda_{dq})^2} - c_1 - c_2\lambda_{dq}\Big) + L_{\mathrm{s}\sigma}L_{\mathrm{r}\sigma}\Big],$$

$$\omega_3 \leftarrow \omega_3(\lambda_{dq}) = R_\mathrm{s}\Big(\sqrt{c_0 + (c_1 + c_2\lambda_{dq})^2} - c_1 - c_2\lambda_{dq}\Big)\Big/\Big[(L_{\mathrm{s}\sigma}+L_{\mathrm{r}\sigma})\cdot\Big(\sqrt{c_0+(c_1+c_2\lambda_{dq})^2} - c_1 - c_2\lambda_{dq}\Big) + L_{\mathrm{s}\sigma}L_{\mathrm{r}\sigma}\Big],$$

$$\omega_4 \leftarrow \omega_4(\lambda_{dq}) = R_\mathrm{r}\Big(\sqrt{c_0 + (c_1 + c_2\lambda_{dq})^2} - c_1 - c_2\lambda_{dq}\Big)\Big/\Big[(L_{\mathrm{s}\sigma}+L_{\mathrm{r}\sigma})\cdot\Big(\sqrt{c_0+(c_1+c_2\lambda_{dq})^2} - c_1 - c_2\lambda_{dq}\Big) + L_{\mathrm{s}\sigma}L_{\mathrm{r}\sigma}\Big],$$

$$\omega_5 \leftarrow \omega_5(\lambda_{dq}) = -R_\mathrm{r}\Big(\sqrt{c_0 + (c_1 + c_2\lambda_{dq})^2} - c_1 - c_2\lambda_{dq} + L_{\mathrm{s}\sigma}\Big)\Big/\Big[(L_{\mathrm{s}\sigma}+L_{\mathrm{r}\sigma})\cdot\Big(\sqrt{c_0+(c_1+c_2\lambda_{dq})^2} - c_1 - c_2\lambda_{dq}\Big) + L_{\mathrm{s}\sigma}L_{\mathrm{r}\sigma}\Big] \qquad (44)$$

mentioning, however, that if a piecewise construct (41) is adopted then the appropriate substitutions

$$c_0 \leftarrow c_{0,k}\,,\quad c_1 \leftarrow c_{1,k}\,,\quad c_2 \leftarrow c_{2,k}$$

have to be made. Emphasising the new flux linkages coefficients, one can straightforwardly find out that the improved structure (42) can be put forward in a form similar to the original one, given by Eqs. (14):

$$(\mathrm{d}\psi_{\mathrm{s}d})/(\mathrm{d}t) = \omega_1(\lambda_{dq})\cdot\psi_{\mathrm{s}d} + \omega_2\,\psi_{\mathrm{s}q} + \omega_3(\lambda_{dq})\cdot\psi_{\mathrm{r}d} + u_{\mathrm{s}d}\,,$$

$$(\mathrm{d}\psi_{\mathrm{s}q})/(\mathrm{d}t) = -\omega_2\,\psi_{\mathrm{s}d} + \omega_1(\lambda_{dq})\cdot\psi_{\mathrm{s}q} + \omega_3(\lambda_{dq})\cdot\psi_{\mathrm{r}q} + u_{\mathrm{s}q}\,,$$

$$\frac{\mathrm{d}\psi_{\mathrm{r}d}}{\mathrm{d}t} = \omega_4(\lambda_{dq})\cdot\psi_{\mathrm{s}d} + \omega_5(\lambda_{dq})\cdot\psi_{\mathrm{r}d} + \omega_6\,\psi_{\mathrm{r}q}\,,$$

$$\frac{\mathrm{d}\psi_{\mathrm{r}q}}{\mathrm{d}t} = \omega_4(\lambda_{dq})\cdot\psi_{\mathrm{s}q} - \omega_6\,\psi_{\mathrm{r}d} + \omega_5(\lambda_{dq})\cdot\psi_{\mathrm{r}q}\,. \qquad (45)$$

4 Dynamic Simulation

The transient selected for validation of the improved structure of flux linkage state-space model has been the switching-in, for grid-connected operation, of a 3.5 kW cage-rotor induction machine having, in per unit (p.u.) system, the following parameters:

$R_\mathrm{s} = 0.0524$ p.u. and $R_\mathrm{r} = 0.0418$ p.u.,

$L_{\mathrm{s}\sigma} = 0.086$ p.u. and $L_{\mathrm{r}\sigma} = 0.1175$ p.u.

The energy for machine magnetization is provided from the power grid in this typical situation. In order to investigate the machine dynamic response, the reference frame fixed to rotor $(\omega_\mathrm{ref} \equiv \omega_\mathrm{r})$ has been considered. The process simulation has been carried out under the initial condition of super-synchronous constant velocity. Therefore, the motion (torque) equation that yields the time-related derivative of the rotor angular velocity, and the linking equation between rotor lead angle and rotor angular velocity [12]-[16] have been added to Eqs. (45).

Notice that the outcomes are all provided in per unit (p.u.) system and that the association of positive signs corresponds to generator operating mode.

4.1 Software Environment

With a view to a fast and highly accurate numerical integration, we had implemented [27] an eight-order Adams-Bashforth scheme (**Appendix B**), a novelty with respect to available data in literature.

The start-up was carried out by the fourth-order Runge-Kutta method [24]-[26]. The small truncation error of the integrator, coupled with a 10-bytes data representation (of type "extended") [27], ensure high numerical integration accuracy.

At each step of numerical integration, the logical sequence of executing the main blocks [27] of the developed software environment is the following:

→ Employment of the Adams-Bashforth scheme in order to update the state vector of the *d*-*q* axis winding flux linkages, having in view the developed form encompassing Eqs. (45):

$$\boldsymbol{\Psi}_{n+1} = \boldsymbol{\Psi}_n + h\sum_{k=n-7}^{n} B_k\,(\boldsymbol{\Omega}_k\boldsymbol{\Psi}_k + \boldsymbol{U}_k)$$

wherein:

$$\boldsymbol{\Psi} = [\psi_{\mathrm{s}d}\ \ \psi_{\mathrm{s}q}\ \ \psi_{\mathrm{r}d}\ \ \psi_{\mathrm{r}q}]^\mathrm{T},$$

$$\boldsymbol{\Omega} = \begin{bmatrix} \omega_1 & \omega_2 & \omega_3 & 0 \\ -\omega_2 & \omega_1 & 0 & \omega_3 \\ \omega_4 & 0 & \omega_5 & \omega_6 \\ 0 & \omega_4 & -\omega_6 & \omega_5 \end{bmatrix},$$

$$\boldsymbol{U} = [u_{\mathrm{s}d}\ \ u_{\mathrm{s}q}\ \ 0\ \ 0]^\mathrm{T};$$

→ Evaluation of quantity (20) that now decides the present value of magnetizing inductance;
→ Updating the magnetizing inductance value by means of the dependency given by Eq. (36);
→ Computation of winding currents by means of currents-flux linkages correlations (24)-(27).

4.2 Depicting Magnetizing Inductance

Fig.1 depicts the machine magnetizing inductance in the traditional manner, i.e. as non-linear dependency on magnetizing current (17). The representation in Fig.1 corresponds to expression (33) of magnetizing inductance, wherein Frölich model parameters are: $\alpha = 0.219$ and $\beta = 0.322$.

Taking now into account the values of the machine leakage inductances, constants (37)-(39) result:

$c_0 = 0.22673981578091167$,

$c_1 = -2.2582770130030404$,

$c_2 = 0.73515981735159817$.

Thus, dependency given by Eq. (36) is established, being also plotted in Fig.2.

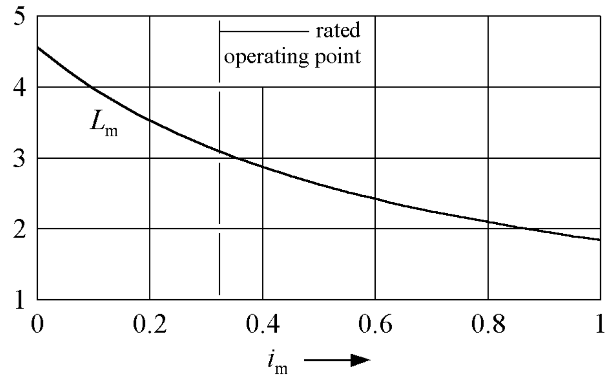

Fig.1: Magnetizing inductance of induction machine utilised in simulation, traditionally given as function of magnetizing current (17).

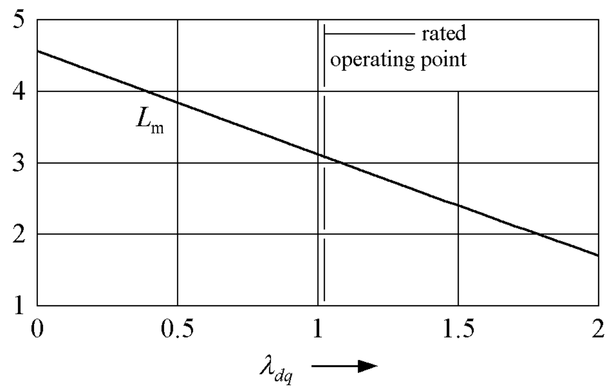

Fig.2: Machine magnetizing inductance, depicted as dependency on flux-dependent quantity (20).

Fig.3 illustrates coefficients (44) as dependencies on quantity (20). Since these coefficients interfere in winding flux linkages derivatives (45), they have to be updated at each step of numerical integration.

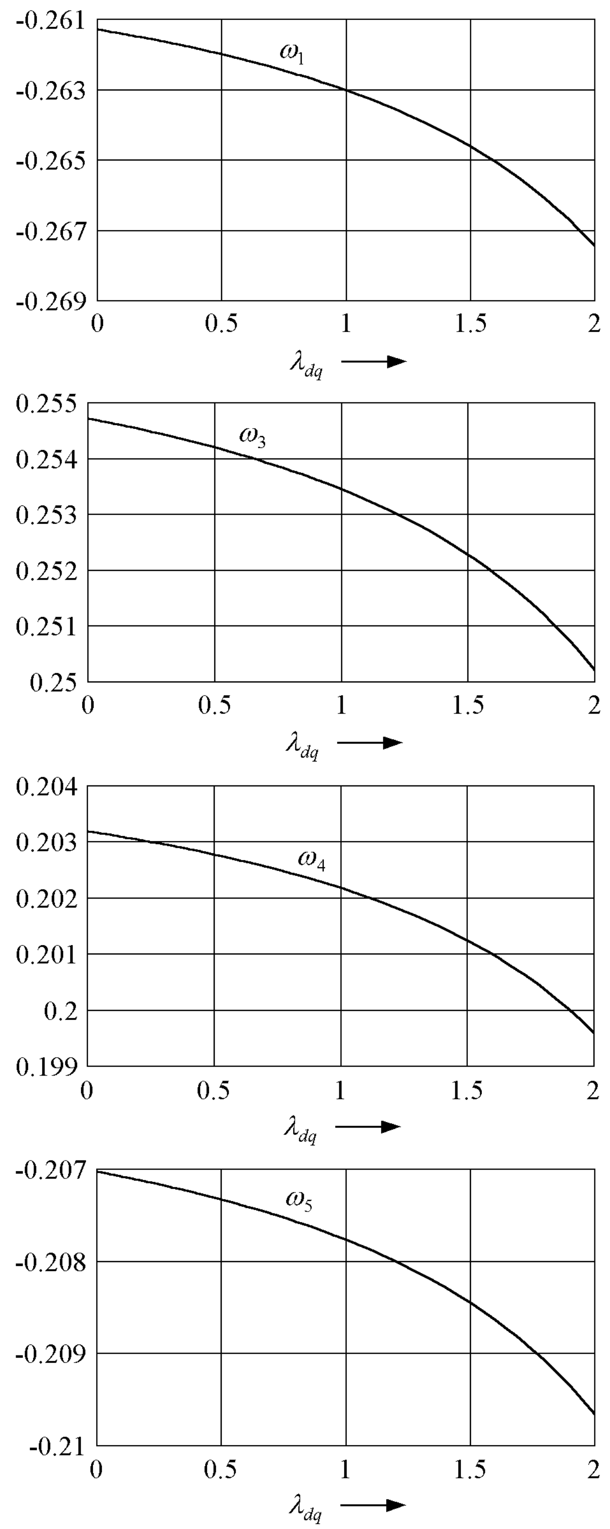

Fig.3: Coefficients (44), which interfere in improved structure (45), depicted (in p.u.) as dependencies on flux-dependent quantity (20).

From the mathematical point of view, the curves shown in Fig.1 and Fig.2 are equivalent. However, while representation shown in Fig.1 requires, in the traditional manner, the magnetizing current (17) as the independent variable, the representation in Fig.2 provides the magnetizing inductance as function of quantity (20), i.e. as function of the *d*-*q* axis winding flux linkages, which are just state variables.

As a consequence, the representation depicted in Fig.2 is to be regarded as a substitute for the original representation, depicted in Fig.1, which traditionally provides the magnetizing inductance as function of magnetizing current (17), i.e. as function of *d*-*q* axis currents. At the same time, the new quantity (20), only expressed in terms of selected state variables, and now deciding the present value of magnetizing inductance, is now to be regarded as a substitute for magnetizing current (17).

4.3 Simulation Results

For the situation corresponding to the switching-in of the 3.5 kW cage-rotor induction machine with the super-synchronous angular velocity of 1.05 p.u., in Fig.4 and Fig.5 are shown the time-related evolution curves of several characteristic quantities.

The dynamic simulation has been carried out in accordance with the assumption of rated power grid r.m.s. voltage and angular frequency. Thus, in the case study here, the machine stator phase voltages, making up a symmetrical system enforced by the power grid, can be described, in the per unit system, by the following expressions:

$$u_{\mathrm{A}} = \sin(\omega_{\mathrm{bus}} t + \alpha_{\mathrm{A}}),$$

$$u_{\mathrm{B}} = \sin(\omega_{\mathrm{bus}} t + \alpha_{\mathrm{A}} - 2\pi/3),$$

$$u_{\mathrm{C}} = \sin(\omega_{\mathrm{bus}} t + \alpha_{\mathrm{A}} - 4\pi/3); \quad \omega_{\mathrm{bus}} \equiv 1\,\text{p.u.}$$

wherefrom, by means of Park-Gorev transform [29], one obtains the *d*-*q* axis voltages, interfering in state equations (45):

$$u_{\mathrm{s}d} = \sin(t + \alpha_{\mathrm{A}} + \gamma_{\mathrm{r}}), \quad u_{\mathrm{s}q} = -\cos(t + \alpha_{\mathrm{A}} + \gamma_{\mathrm{r}}) \qquad (46)$$

with γ_{r} as the rotor lead angle.

For the circumstance corresponding to $\alpha_{\mathrm{A}} = 0$ in Eqs. (46), Fig.4 depicts the quantities usually used to assess the switching-in transient. The peak values of stator currents through phases A and B occur at the first pulse, while the peak value of the phase C current occurs at the second pulse. More precisely, the peak values of the phase A and phase B currents are 5.6714 p.u. (absolute value) and 4.9811 p.u., and occur at instant 2.82 rad. and 1.8 rad., respectively. In contrast, the first pulse of phase C current occurs at the instant 0.96 rad., however the peak value of 4.0572 p.u. being reached at 4.08 rad. At a later instant, the machine electromagnetic torque, plotted in Fig.4(d), reaches the peak value of 2.0781 p.u.

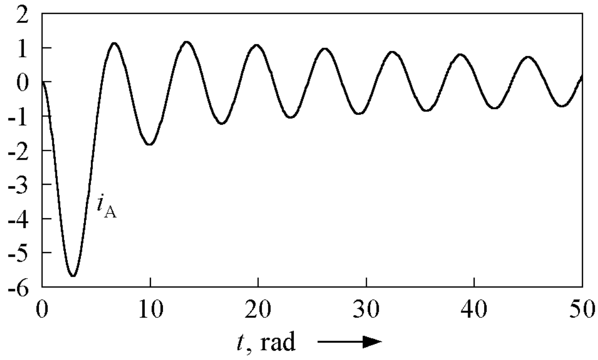

Fig.4(a) Stator phase A current

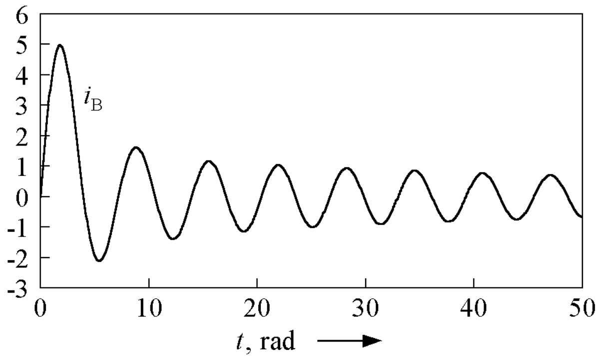

Fig.4(b) Stator phase B current

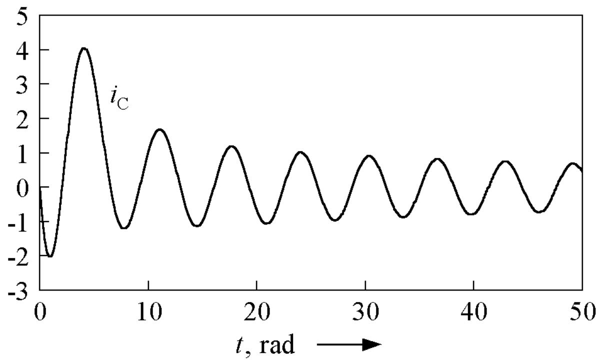

Fig.4(c) Stator phase C current

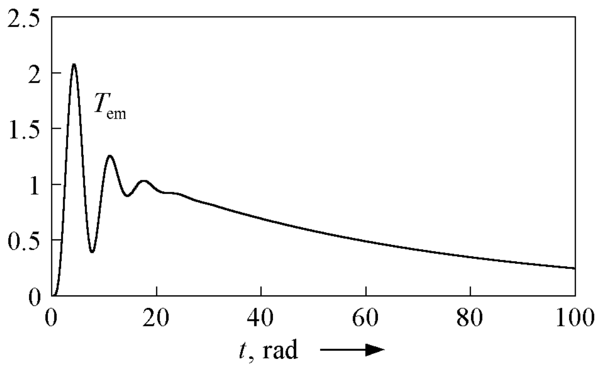

Fig.4(d) Electromagnetic torque

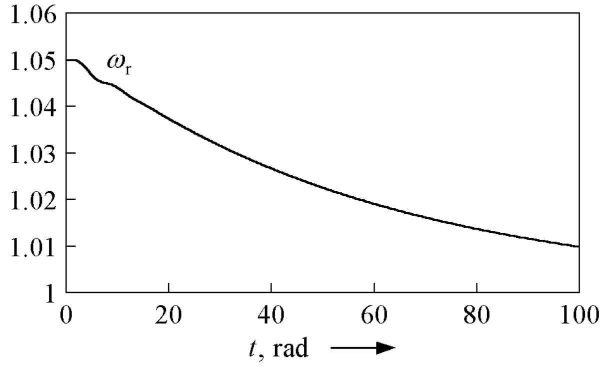

Fig.4(e) Rotor angular velocity

Fig.4: The time-related curves of the characteristic quantities at switching-in of the 3.5 kW cage-rotor induction machine.

Fig.5 displays the time-related curves of quantities in connection with magnetizing circuit. The set of curves in Fig.5(a)-(c) wholly depicts the behaviour of machine magnetizing circuit. The curves merged in Fig.5(d) point out the effects of the variation of magnetic stress on the non-linearity extent of state equations (45). Moreover, Fig.5(c) clearly indicates that the time-related curves of magnetizing current and of flux-dependent quantity (20) take the same shape. Besides, both quantities in Fig.5(c) increase rapidly up to their peak values, which correspond to an under-rated magnetizing inductance (Fig.5(b)).

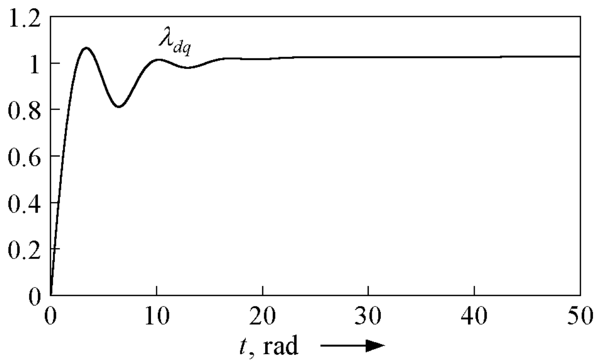

Fig.5(a) Flux-dependent quantity (20)

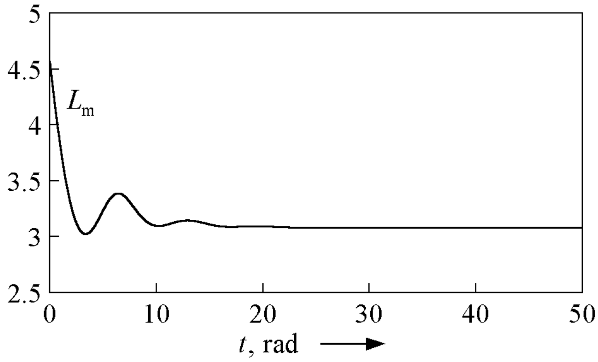

Fig.5(b) Magnetizing inductance

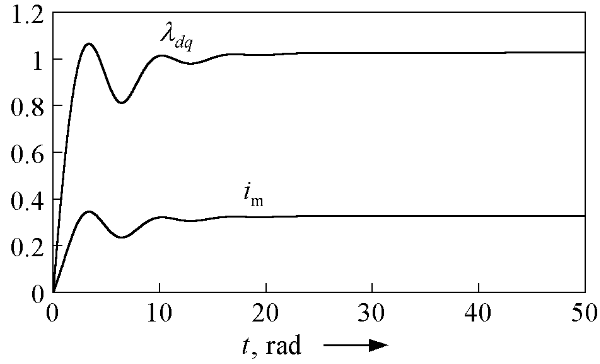

Fig.5(c) Flux-dependent quantity (20) together with magnetizing current

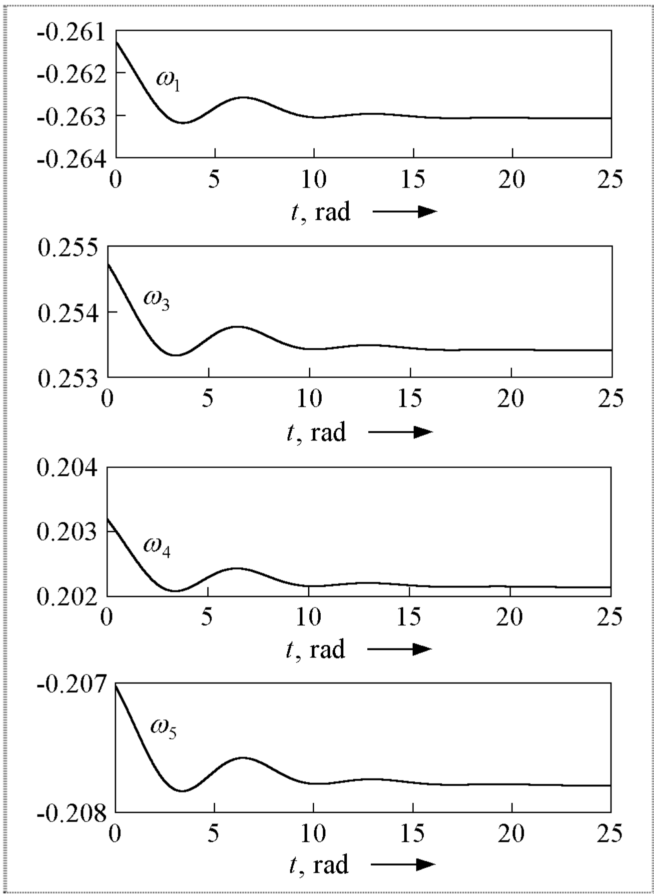

Fig.5(d) Coefficients (44) in improved structure (45)

Fig.5: Evolution of the quantities in connection with magnetizing circuit, occurring at switching-in of the 3.5 kW cage-rotor induction machine.

Since the magnetizing curve is provided here by means of a differentiable function of magnetizing current variable, i.e. function (32), all the additional saturation-dependent parameters that interfere in the well-established structure of winding current state-space model (developed by selecting all the *d*-*q* axis winding currents as state variables) can be computed [14], [17], [18]. The computation of each additional parameter in the compass of the structure of winding current state-space model asks for the present value of dynamic (differential) inductance:

$$L = L(i_{\mathrm{m}}) = \frac{\mathrm{d}\,\psi_{\mathrm{m}}}{\mathrm{d}\,i_{\mathrm{m}}} \,. \qquad (47)$$

For instance, the well-known saturation-dependent crosscoupling inductance of winding current state-space model, namely:

$$L_{dq} = (L - L_{\mathrm{m}})\,(i_{\mathrm{s}d} + i_{\mathrm{r}d})\,(i_{\mathrm{s}q} + i_{\mathrm{r}q}) \big/ i_{\mathrm{m}}^2$$

is just at hand since, in our case study, the dynamic inductance (47) gets the expression:

$$L = \frac{\mathrm{d}}{\mathrm{d}\,i_{\mathrm{m}}}\left(\frac{i_{\mathrm{m}}}{\alpha + \beta i_{\mathrm{m}}}\right) = \alpha \big/ (\alpha + \beta i_{\mathrm{m}})^2 \,.$$

Thus, the winding current state-space model being usable, it has to be emphasised that its employment has led to simulation results identical to those in Fig.4, previously discussed. A zoomed-in picture of results received by application of winding current state-space model is presented in Fig.6.

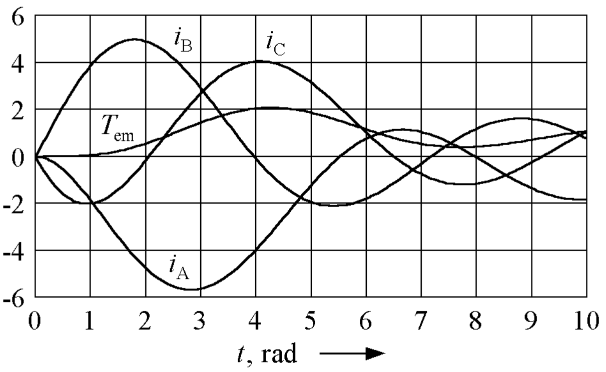

Fig.6: Switching-in simulation results, received by application of winding current state-space model.

5 Discussion and Conclusions

Induction machine is now operated in the immediate nearness of the security limits and, thus, is exposed to large variations of magnetic stress. Having this in view, the present paper advances an effecting and accurate procedure of improving the winding flux linkage state-space model of induction machine by including the main flux saturation effects. Tending towards a method of magnetizing inductance on-line updating, we placed the emphasis on the necessity of replacing the magnetizing current, given in terms of *d*-*q* axis currents, by a quantity only expressed in terms of winding flux linkages. In opposition to the research works already stated in literature, the *d*-*q* axis currents in magnetizing current expression have been here replaced by flux-based expressions. Such a manipulation made feasible the formulation of an auxiliary algebraic equation suitable for solving in relation to magnetizing inductance as being here the only saturation-dependent machine parameter. We found that the employment of the well-established Frölich model to describe the machine magnetizing curve causes the auxiliary equation to change to a second order algebraic one. As a result of symbolic solving of this particular equation, the magnetizing inductance comes forth as function of only *d*-*q* axis winding flux linkages, which are just state variables of original structure of winding flux linkage state-space model. Thus, the sole intervention the system analysts have to perform into the original structure of the winding flux linkage state-space model is to substitute the magnetizing inductance, being there constant parameter, by expression (36) in the paper.

The formulation of the auxiliary equation has been carried out without altering the generalised *d*-*q* axis mathematical model of the induction machine. Consequently, although incorporating the main flux saturation effects, the improved structure possesses both the structural simplicity of original flux linkage state-space model and the intrinsic accuracy of the commonly accepted picture of induction machine. Besides, as it solely involves elementary algebraic operations, the evaluation of (algebraic) expression (36) is not very time consuming for on-line updating of magnetizing inductance, so that if the main flux saturation level varies, the improved model keeps track of this variation. Thus, the improved model is prepared for integration into software environments dedicated for power systems on-line assessment.

Furthermore, since the dynamic inductance does not interfere, magnetizing curve fitting can easily be controlled by employing Frölich type model (32) to describe each piece of a piecewise representation. In this case, magnetizing inductance is to be computed also by means of a piecewise representation, with the mention that each piecewise segment has to be described by means of a non-linearity of type (36).

Although of easy accessibility and accurate, the derivation is validated by performing the dynamic simulation of an induction machine switching-in to the effect of grid-connected operating. The detailed case study here indicates that the improved winding flux linkage state-space model leads to the same results as the existing winding current state-space model also applied in conjunction with Frölich type model of anhysteretic magnetizing curve. Moreover, the results received from the model developed in the paper clearly indicate that the time-related curves of magnetizing current and quantity (20) take the same shape. Therefore, we may conclude that, besides the magnetizing current (17), the new quantity (20) also intimates the saturation level of the main flux path.

6 List of Main Symbols

u	instantaneous voltage;
i	instantaneous current;
ψ	instantaneous flux linkage;
R	resistance;
L	inductance;
ω	angular velocity; coefficient in structure of winding flux linkage state-space model;
t	time variable;
α, β	Frölich model parameters;
λ_{dq}	quantity connected with *d*-*q* axis winding flux linkages, deciding the present value of magnetizing inductance, i.e. quantity that acts as a substitute for magnetizing current;
f	function pointing a quantity (magnetizing inductance, *d*- or *q*-axis winding current) connected with and varying with *d*-*q* axis winding flux linkages;
g	function pointing the magnetizing current as quantity connected with and varying with magnetizing inductance;
c	constants of value decided by the leakage inductances and Frölich model parameters;

Sub-/Super-scripts:

s, r	variables and parameters associated with stator and rotor, respectively;
m	variables and parameters associated with main flux path (magnetizing circuit);
σ	suffix to denote leakage inductances;
d	suffix to denote *d*-axis components;
q	suffix to denote *q*-axis components;
k	index;
T	transposed vector.

Appendix A

Replacing the stator *d*-*q* axis currents in generalised expression (9), using correlations (24) and (25), we eventually get the electromagnetic torque expression in terms of only *d*-*q* axis winding flux linkages:

$$T_{\mathrm{em}} = \frac{3p}{2}\,\frac{f(\lambda_{dq})\cdot(\psi_{\mathrm{s}q}\,\psi_{\mathrm{r}d} - \psi_{\mathrm{s}d}\,\psi_{\mathrm{r}q})}{(L_{\mathrm{s}\sigma}+L_{\mathrm{r}\sigma})\cdot f(\lambda_{dq}) + L_{\mathrm{s}\sigma}L_{\mathrm{r}\sigma}}$$

with the main flux saturation effects to be included straightforwardly, i.e. by means of dependency (36), or by means of a piecewise construct, given by (41). Having in view that (41) is composed only of pieces of the type (36), we may expand:

$$T_{\mathrm{em}} = \frac{3p}{2}\Bigg[\left(\sqrt{c_0 + (c_1 + c_2\lambda_{dq})^2} - c_1 - c_2\lambda_{dq}\right) \cdot(\psi_{\mathrm{s}q}\,\psi_{\mathrm{r}d} - \psi_{\mathrm{s}d}\,\psi_{\mathrm{r}q})\Big]\Big/\Big[(L_{\mathrm{s}\sigma}+L_{\mathrm{r}\sigma}) \cdot\left(\sqrt{c_0 + (c_1 + c_2\lambda_{dq})^2} - c_1 - c_2\lambda_{dq}\right) + L_{\mathrm{s}\sigma}L_{\mathrm{r}\sigma}\Bigg],$$

with the mention that if a piecewise representation (41) is adopted then the appropriate substitutions

$$c_0 \leftarrow c_{0,k}, \quad c_1 \leftarrow c_{1,k}, \quad c_2 \leftarrow c_{2,k}$$

have to be performed in the previous expression. It has to be emphasised that, in per unit (p.u.) system, the expression of machine electromagnetic torque does not include the coefficient $\frac{3p}{2}$.

Appendix B

For the ODE of the general form:

$$\frac{\mathrm{d}\psi}{\mathrm{d}t} = \varphi(t, \psi),$$

the eight-order Adams-Bashforth scheme [24], [25] gets the specific form:

$$\psi_{n+1} = \psi_n + h\sum_{k=n-7}^{n} B_k\,\varphi(t_k, \psi_k)$$

with h as the integration stepsize. For $k \in [n-7, n]$, we have obtained [30]:

$$B_k = \frac{(-1)^{n-k}}{[(k-n+7)!]\,[(n-k)!]}\int_0^1 \frac{(\tau+7)\ldots\tau}{\tau+n-k}\,\mathrm{d}\tau,$$

that is:

$$B_{n-7} = -\frac{36799}{120960}, \qquad B_{n-6} = \frac{295767}{120960},$$

$$B_{n-5} = -\frac{1041723}{120960}, \qquad B_{n-4} = \frac{2102243}{120960},$$

$$B_{n-3} = -\frac{2664477}{120960}, \qquad B_{n-2} = \frac{2183877}{120960},$$

$$B_{n-1} = -\frac{1152169}{120960}, \qquad B_n = \frac{434241}{120960}.$$

The source code of Delphi.NET/FreePascal unit that implements the eight-order integrator is given next. We have designed the unit with the main purpose of maximizing execution speed.

```
UNIT online_integrator;
   // fast eight-order Adams-Bashforth integrator
   // Delphi source file: online_integrator.pas

INTERFACE
type  vector = array[byte] of extended;
var   num_of_statevar: byte;
          // number of state variables
      h: extended;     // integration stepsize
      t: extended;     // time variable
      tend: extended;
          // ending value of time variable
statevar: vector;
          // state variables vector
```

```
statevarder: vector;
    // vector of state variables derivatives
compute_statevar_derivatives: procedure;
    // yields the state variables derivatives as
    // expressions in terms of state variables
startup: procedure;
    // seven Runge-Kutta steps; vector statevarder7 is
    // not to be computed within this procedure
compute_quanti: procedure;
    // yields the characteristic quantities as
    // functions of state variables statevar[i]
procedure ab8;
    // the eight-order Adams-Bashforth scheme

IMPLEMENTATION
const  b0: extended = - 36799.0 / 120960.0;
       b1: extended = 295767.0 / 120960.0;
       b2: extended = - 1041723.0 / 120960.0;
       b3: extended = 2102243.0 / 120960.0;
       b4: extended = - 2664477.0 / 120960.0;
       b5: extended = 2183877.0 / 120960.0;
       b6: extended = - 1152169.0 / 120960.0;
       b7: extended = 434241.0 / 120960.0;
              // Adams-Bashforth coefficients
var    i: byte;
       h_b0, h_b1, h_b2, h_b3, h_b4,
       h_b5, h_b6, h_b7: extended;
              // Adams-Bashforth coefficients
              // multiplied by the stepsize h
       statevarder0, statevarder1, statevarder2,
       statevarder3, statevarder4, statevarder5,
       statevarder6, statevarder7: vector;
           // memorize state variables derivatives
           // at eight successive integration steps

procedure multiplication;
    // multiplies Adams-Bashforth coefficients
    // by the stepsize h
begin
    h_b0 := h * b0; h_b1 := h * b1; h_b2 := h * b2;
    h_b3 := h * b3; h_b4 := h * b4; h_b5 := h * b5;
    h_b6 := h * b6; h_b7 := h * b7
end;  // multiplication

procedure onestep_adamsbashforth8;
var    m0, m1, m2, m3, m4,
       m5, m6, m7: extended;
begin
    // memorize the present values of
    // the state variables derivatives
    compute_statevar_derivatives;
           // yields the vector statevarder for present
           // values statevar[i] of state variables
    for i := 1 to num_of_statevar do
        statevarder7[i] := statevarder[i];
    // update state variables and
    // vectors statevarder0 ... statevarder6
    t := t + h;     // updates time variable
    for i := 1 to num_of_statevar do begin
        m0 := statevarder0[i]; m1 := statevarder1[i];
        m2 := statevarder2[i]; m3 := statevarder3[i];
        m4 := statevarder4[i]; m5 := statevarder5[i];
        m6 := statevarder6[i]; m7 := statevarder7[i];
        // Adams-Bashforth scheme to update
        // the state variable of index i
        statevar[i] := statevar[i]
            + h_b0 * m0 + h_b1 * m1 + h_b2 * m2
            + h_b3 * m3 + h_b4 * m4 + h_b5 * m5
            + h_b6 * m6 + h_b7 * m7;
        // update statevarder0[i] ... statevarder6[i]
        statevarder0[i] := m1;
                  // statevarder0 is lost
        statevarder1[i] := m2; statevarder2[i] := m3;
        statevarder3[i] := m4; statevarder4[i] := m5;
        statevarder5[i] := m6; statevarder6[i] := m7
                  // transfer
    end;
    compute_quanti
end;  // onestep_adamsbashforth8

procedure ab8;
begin
    multiplication;
    startup;
    repeat
        onestep_adamsbashforth8
    until t >= tend;
end;  // ab8

end.  // UNIT online_integrator
```


References:

[1] P.C. Fusaro, *Energy Risk Management*, McGraw-Hill, New York, 1998.

[2] A. Karami, M. Rashidinejad, A.A. Gharaveisi, Coordination of UPFC & SVC for voltage security enhancement, *WSEAS Transactions on Power Systems*, Vol.1, No.5, 2006, pp. 740-746.

[3] M. Taleb, S. Ahmed-Zaid, W.W. Price, Induction machine models near voltage collapse, *Electric Machines and Power Systems*, Vol.25, No.1, 1997, pp. 15-28.

[4] H. Bentarzi, L. Refoufi, F.Z. Dekhandji, New approach of induction motor performance study under different voltage unbalance conditions, *WSEAS Transactions on Power Systems*, Vol.1, No.8, 2006, pp. 1519-1525.

[5] D.S. Zinger, E. Muljadi, Annualized wind energy improvement using variable-speed, *IEEE Transactions on Industry Applications*, Vol.33, No.6, 1997, pp. 1444-1447.

[6] A.F. Silva, F.A. Castro, J.N. Fidalgo, A neural network control strategy for improved energy capture on a variable-speed wind turbine, *WSEAS Transactions on Information Science & Applications*, Vol.2, No.5, 2005, pp. 450-454.

[7] M.R. Patel, *Wind and Solar Power Systems*, CRC Press, Boca Raton, 1999.

[8] Y. Tsukamoto, J. Sugimoto, R. Yokoyama, Y. Zhou, Economic evaluation and scenario analysis of wind generations based on environment factors, *WSEAS Transactions on Power Systems*, Vol.1, No.8, 2006, pp. 1526-1531.

[9] K. Ichiyanagi, K. Taniguchi, K. Yukita, Y. Goto, K. Mizuno, Y. Hoshino, N. Yamamoto, S. Sugimoto, Forecasting of wind power variation by using AMeDAS data and pattern matching of weather map, *WSEAS Transactions on Power Systems*, Vol.1, No.12, 2006, pp. 2023-2028.

[10] M.E. El-Hawary, *Electrical Energy Systems*, CRC Press, Boca Raton, 2000, Ch.8 (The energy control center).

[11] E. Levi, V. Vuckovic, Magnetizing curve representation methods in digital simulation of induction machine dynamics, *International Journal of Modelling and Simulation*, Vol.10, No.2, 1990, pp. 52-56.

[12] I. Boldea, *Electric Machine Parameters* (in Romanian), Publishing House of Romanian Academy, Bucharest, 1991.

[13] I. Boldea, S.A. Nasar, A unified analysis of magnetic saturation in orthogonal axis models of electrical machines, *Electric Machines and Power Systems*, Vol.12, No.3, 1987, pp. 195-204.

[14] I. Boldea, S.A. Nasar, *The Induction Machine Handbook*, CRC Press, Boca Raton, 2002.

[15] R.J. Kerkman, Steady-state and transient analysis of an induction machine with saturation of the magnetizing branch, *IEEE Transactions on Industry Applications*, Vol.21, No.1, 1985, pp. 226-234.

[16] E. Levi, Z. Krzeminski, Main flux-saturation modelling in *d-q* axis models of induction machines using mixed current-flux state-space models, *European Transactions on Electrical Power*, Vol.6, No.3, 1996, pp. 207-215.

[17] J.E. Brown, K.P. Kovacs, P. Vas, A method of including the effects of main flux path saturation in the generalized equations of AC machines, *IEEE Transactions on Power Apparatus and Systems*, Vol.102, No.1, 1983, pp. 96-103.

[18] P. Vas, Generalized analysis of saturated AC machines, *Archiv für Elektrotechnik*, Vol.64, No.1-2, 1981, pp. 57-62.

[19] L. Lupsa-Tataru, Generalised method of completing the flux linkage state-space model of induction machine to include the effects of main flux saturation, *WSEAS Transactions on Power Systems*, Vol.2, No.2, 2007, pp. 35-40.

[20] L. Lupsa-Tataru, An extension of flux linkage state-space model of synchronous generators with a view to dynamic simulation, *WSEAS Transactions on Power Systems*, Vol.1, No.12, 2006, pp. 2017-2022.

[21] R.M. Bozorth, *Ferromagnetism*, Wiley-IEEE Press, New York, 1993.

[22] R.M. Bozorth, *Ferromagnetism*, IEEE Press, New York, 1978.

[23] J. Stepina, Space-phasor theory? – What is that for? (Letter to the Editor), *European Transactions on Electrical Power*, Vol.5, No.6, 1995, pp. 409-412.

[24] W.H. Press, B.P. Flannery, S.A. Teukolsky, W.T. Vetterling, *Numerical Recipes in Fortran: The Art of Scientific Computing*, 2nd ed., Cambridge University Press, England, 1992.

[25] H. Jeffreys, B.S. Jeffreys, *Methods of Mathematical Physics*, 3rd ed., Cambridge University Press, England, 1988.

[26] C.W. Gear, *Numerical Initial Value Problems in Ordinary Differential Equations*, Prentice-Hall, Englewood Cliffs, 1971.

[27] www.freepascal.org: FreePascal Integrated Development Environment for Win32/64 (Compiler v.2.2.0 for Delphi 7).

[28] www.borland.com: *Delphi Language Guide*, Borland Software Corporation, Scotts Valley, California, 2004.

[29] A.A. Gorev, *Transient Processes of Synchronous Machine* (in Russian), Nauka, Sankt-Petersburg, 1985.

[30] L. Lupsa-Tataru, *Transients in Synchronous Machines: Modelling and Dynamic Simulation* (in Romanian), Transilvania University Press, Brasov, 2007, ISBN 978-973-635-953-8, pp. 95-108.